The tethered configuration of the EGF receptor extracellular domain exerts only a limited control of receptor function

Dawn Mattoon*, Peter Klein*†, Mark A. Lemmon‡, Irit Lax*, and Joseph Schlessinger*§

*Department of Pharmacology, Yale University School of Medicine, 333 Cedar Street, New Haven, CT 06520; †Fox Run Management, LLC, 35 Fox Run Lane, Greenwich, CT 06831; and ‡Department of Biochemistry and Biophysics, University of Pennsylvania School of Medicine, Philadelphia, PA 19104

Contributed by Joseph Schlessinger, November 26, 2003

Quantitative epidermal growth factor (EGF)-binding experiments have shown that the EGF-receptor (EGFR) is displayed on the surface of intact cells in two forms, a minority of high-affinity and a majority of low-affinity EGFRs. On the basis of the three-dimensional structure of the extracellular ligand binding domain of the EGFR, it was proposed that the intramolecularly tethered and autoinhibited configuration corresponds to the low-affinity receptor, whereas the extended configuration accounts for the high-affinity EGFRs on intact cells. Here we test this model by analyzing the properties of EGFRs mutated in the specific regions responsible for receptor autoinhibition and dimerization, respectively. Our results show that mutagenic disruption of the autoinhibitory tether in EGFR results in a decrease in the dissociation rate of EGF without a detectable change in EGFR activation and signaling through EGFR even in response to stimulation with low concentrations of EGF. Mutagenic disruption of the dimerization arm, on the other hand, increased the rate of EGF dissociation and impaired EGFR activation and signaling via the EGFR. This study demonstrates that the extended configuration of EGFR does not account for the apparent high-affinity EGF-binding to EGFR on intact cells. Furthermore, the autoinhibition conferred by the tethered configuration of the extracellular ligand-binding domain provides only a limited control of EGFR function.

The multiple members of the epidermal growth factor (EGF) family of polypeptide growth factors mediate their diverse array of cellular responses by binding to and activating a family of four receptor tyrosine kinases designated EGF-receptor (EGFR), ErbB2, -3, and -4. A large body of experimental evidence has revealed the importance of both ligands and receptor families in mediating a variety of critical processes during embryogenesis as well as in numerous adult tissues and organs (reviewed in ref. 1). The EGFR and the signaling pathways that are activated in response to ligand-stimulation are conserved from nematode to humans, underscoring the biological importance of this pathway. Furthermore, a variety of cancers (i.e., squamus carcinoma, glioblastoma) and other diseases are caused by dysfunctions in this family of receptors or in their downstream effector proteins (2).

Quantitative studies of EGF binding to intact cells have demonstrated that EGFRs exist on the surface in two different affinity classes; a majority (95–98%) of low-affinity (K_D = 2–5 nM), and a minority (2–5%) of high-affinity (K_D = 10–100 pM) EGF receptors (3). The existence of these two affinity states is suggested by Scatchard analysis of ^{125}I-labeled EGF (^{125}I-EGF) binding data, which typically produces concave-up curvilinear plots. The initial steep slope of these plots is thought to correspond to the high-affinity form of the EGFR, whereas the shallow slope corresponds to the low-affinity form of EGFR. It is important to note however, that these slopes represent only apparent affinities, and do not directly measure molecular binding events. A variety of mechanisms have been proposed for the control of high-affinity ligand binding by the EGFR, including receptor oligomerization, conformational changes in the receptor molecule, and interactions with heterologous membrane or cytoplasmic proteins or other molecules (1, 4).

The intrinsic protein tyrosine kinase activity of the EGFR is activated by EGF-stimulation of receptor dimerization, resulting in autophosphorylation of the cytoplasmic domain of EGFR on multiple tyrosine residues. The autophosphorylation sites serve as binding sites for the Src homology 2 (SH2) and phosphotyrosine-binding (PTB) domains of signaling proteins that are recruited to the receptor after ligand-stimulation, enabling signal transmission to a variety of intracellular compartments to initiate cell proliferation, differentiation, cell survival, and cell locomotion (5).

X-ray crystal structures of the extracellular regions of the EGFR and ErbB3 argue that, before ligand stimulation, the majority of the receptors exist on the cell surface in an autoinhibited or tethered configuration. In this configuration, intramolecular-specific contacts between a ''dimerization arm'' in domain II and an homologous region in domain IV constrain the relative orientations of the two regions responsible for ligand binding (domains I and III) so they cannot both contact the ligand simultaneously (6, 7). It is thought that this tethered autoinhibited state is in a dynamic equilibrium with extended forms of EGFR in which the dimerization arm of each protomer is free to make contacts with an adjoining receptor to mediate EGFR dimerization (4, 7–10). EGF binds preferentially to the extended forms of the receptor (where domains I and III can both contact the ligand), shifting the equilibrium toward dimerization, resulting in autophosphorylation and stimulation of protein tyrosine kinase activity. Thus, it has been hypothesized that the tethered configuration of EGFR may represent the low-affinity EGF binding sites observed in Scatchard plots, whereas the extended dimeric configuration is responsible for high-affinity EGF binding sites on intact cells (4, 6–10).

In this report and the accompanying manuscript (11), we test this hypothesis by analyzing the ligand-binding characteristics of and cell signaling via EGFR mutants in which the intramolecular tether or receptor dimerization were specifically disrupted. We find that the two configurations of the EGFR extracellular region cannot account for the high and low-affinity classes of EGF binding sites expressed on the surface of intact cells on the basis of experimental and theoretical grounds (11). By studying the signaling properties of the same mutants, we also find that the intramolecular domain II/IV tether provides only a limited control of EGF binding, EGFR activation, and cell signaling. We conclude that the inactive state of the EGFR must be maintained by additional autoinhibitory mechanisms that complement the limited autoinhibition exerted by the extracellular domain.

Abbreviations: EGF, epidermal growth factor; EGFR, EGF receptor; MAPK, mitogen-activated protein kinase; ^{125}I-EGF, ^{125}I-labeled EGF.

§To whom correspondence should be addressed. E-mail: joseph.schlessinger@yale.edu.

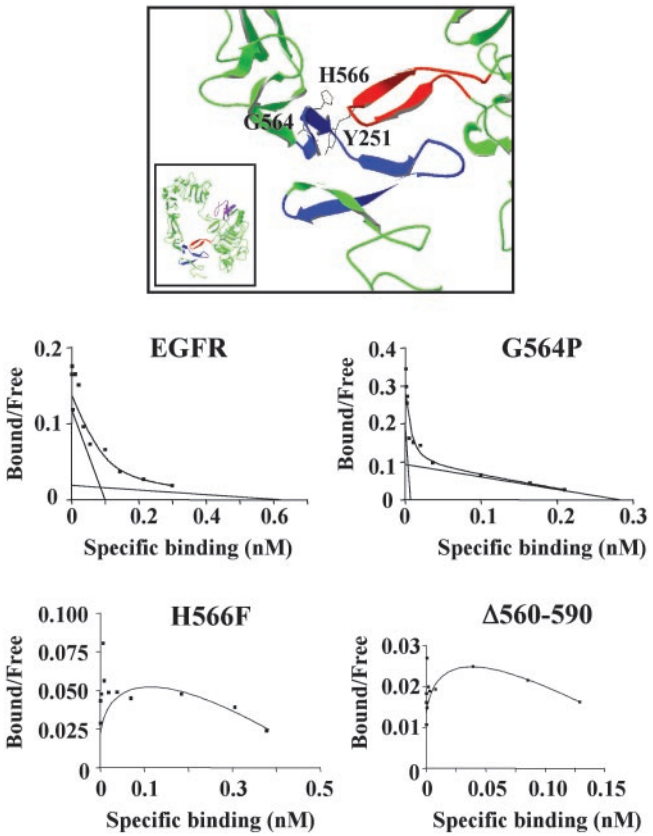

Fig. 1. EGF-binding characteristics of the EGFR mutated in the autoinhibitory tether region. Cells expressing wild-type EGFR or receptors containing mutations in the autoinhibitory portion of domain IV were grown to confluence in 24-well plates and incubated with increasing concentrations of ^{125}I-EGF in triplicate for 60 min at room temperature. A 100-fold excess of unlabeled EGF was simultaneously added to the third well to determine nonspecific binding. Scatchard plots are shown for cell lines expressing wild-type EGFR, G564P, H566F, and the Δ560-590 deletion EGFR mutant. Mutation of G564 to proline produced a Scatchard plot similar to wild type, with two apparent affinity classes. Mutation of H566 to phenylalanine or deletion of residues 560–590 led to a significant alteration in the Scatchard curves that is inconsistent with two EGF-binding affinity classes. A ribbon diagram of the crystal structure of the autoinhibitory portion of domain IV of the EGFR is shown (*Top*), as is the complete monomeric autoinhibited EGFR extracellular domain crystal structure (*Inset*). The dimerization arm of domain II (residues 242–259) is shown in red, and the autoinhibitory region (residues 560–590) is shown in blue (structural coordinates, PDB accession number 1NQL; ref. 7).

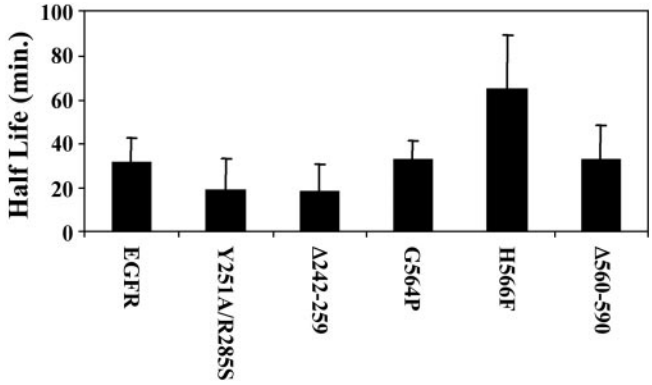

Fig. 2. Dissociation rates of EGF from wild-type or mutant EGF receptors. Cells expressing wild-type EGFR or receptors containing mutations in the dimerization arm of domain II or the autonihibitory tether in domain IV were grown to confluence in 24-well plates and incubated with a single concentration of ^{125}I-EGF in duplicate for 2.5 h at 4°C. EGF was then allowed to dissociate at 4°C for various periods of time ranging from 2 min to 3 h. Dissociation rates were calculated by using one-phase exponential decay. The average of five independent experiments is shown for each receptor.

Materials and Methods

Constructs and Cell Lines. The wild-type EGFR cloned into the retroviral LXSN vector was a gift from David Stern (Yale University, New Haven, CT). Point mutants were generated by single-step site-directed mutagenesis according to the manufacturer's instructions (Stratagene). The EGFR deletion mutant Δ242-259 was generated in two steps in which residues 242–252 were deleted in the first step, followed by residues 253–259. The EGFR deletion mutant Δ560-590 was generated in three steps: removal of residues 573–581, followed by removal of residues 582–590, and removal of amino acids 560–572. GPG cells (gift of Joan Brugge, Harvard University, Cambridge, MA) were transfected with 12 μg of each of these plasmids by using lipofectamine (Gibco) according to the manufacturers' specifications. Harvested virus was used to infect 2.2 cells as described (12). Stable cell lines were generated by selecting infected cells in 800 μg/ml G418 (Gibco). Pools of selected cells were then subcloned and matched for receptor expression level. Cells were maintained in DMEM supplemented with 10% calf serum (Gibco), 100 units/ml penicillin/streptomycin (Gibco), and 400 μg/ml G418.

Immunoprecipitation and Immunoblotting. Cells were grown on 15-cm plates as described above to ≈80% confluence and then starved overnight in DMEM without serum. Cells were left unstimulated or were stimulated with recombinant human EGF (Invitrogen) as indicated. Stimulations were halted with the addition of ice-cold PBS. Cells were washed in PBS and lysed in buffer containing 1% Triton X-100 as described (13). For EGFR immunoprecipitations, anti-EGFR monoclonal antibody 108 (12) was added, and extracts were incubated overnight at 4°C with rotation. Protein A Sepharose (Zymed) was added to immunoprecipitates and incubated for 1 h at 4°C. Immunoprecipitates were then washed in buffer containing 0.1% Triton X-100, separated by SDS/PAGE, and transferred to nitrocellulose membranes (Bio-Rad). For mitogen-activated protein kinase (MAPK) and AKT immunoblotting, total cell extracts were separated directly by SDS/PAGE and transferred to nitrocellulose membranes. Membranes were blocked for 1 h or overnight in 5% BSA/TBS and immunoblotted as indicated. Antiphosphotyrosine blotting was carried out with a mixture of antiphosphotyrosine (P-Tyr) antibodies 4G10 (Upstate Biotechnology), PY20 (Cell Signaling Technology), and monoclonal antibody 72 (13). Anti-EGFR blotting was performed with anti-human EGFR polyclonal antibody (Santa Cruz Biotechnology). MAPK p42/44 and AKT immunoblotting were performed with polyclonal antibodies (Cell Signaling Technology). Proteins were visualized by incubation with Enhanced Chemiluminescence (Amersham Pharmacia) according to the manufacturer's specifications.

^{125}I-EGF Binding Experiments. Cells were plated on 24-well plates and allowed to grow to confluence (≈48 h) in DMEM supplemented with 10% calf serum. Cells from two wells were counted for use in determining receptor number per cell in Scatchard analysis. Cells were washed twice in cold DMEM containing 0.1% BSA at 4°C. EGF was iodinated by using the chloramine T method to 100,000–250,000 cpm/ng (^{125}I from Perkin–Elmer). Triplicate wells were treated with ^{125}I-EGF at concentrations ranging from 0.1 to 100 ng/ml. A 100-fold excess of unlabeled EGF was added to the third well at each concentration and

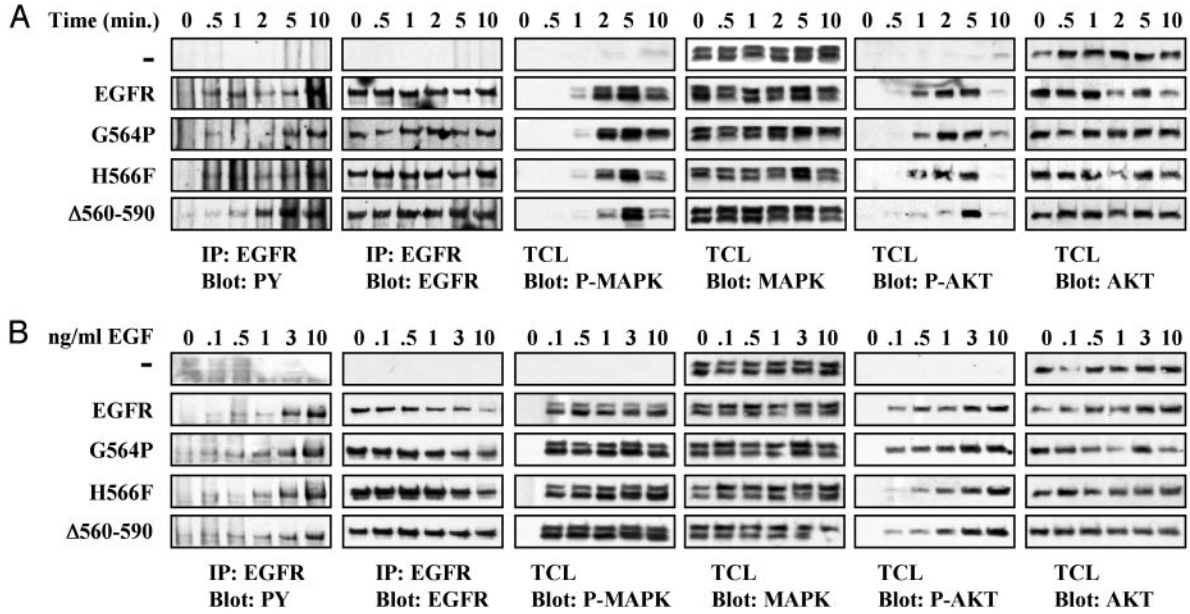

Fig. 3. Signaling and activation of the EGFR mutated in the autoinhibitory tether. (*A*) Cells expressing empty vector (−), wild-type EGFR or the domain IV mutants G564P, H566F, and the Δ560-590 deletion mutant were starved overnight, and stimulated with 1 ng/ml EGF for increasing periods of time. Cell extracts were prepared and analyzed for tyrosine autophosphorylation of EGFR and for activation of MAPK and AKT by using antibodies that recognize specifically the activated forms of MAPK or AKT, respectively. Mutagenic disruption of the autoinhibitory portion of domain IV did not dramatically alter the kinetics of tyrosine autophosphorylation of EGFR or MAPK and AKT activation. (*B*) Cells expressing empty vector (−), wild-type EGFR or the domain IV mutants G564P, H566F, and the Δ560-590 deletion mutant were starved overnight, and stimulated with increasing concentrations of EGF for 5 min at 37°C. Cell extracts were prepared and analyzed for tyrosine autophosphorylation of EGFR and for MAPK and AKT activation. Wild-type EGFR and the domain IV mutants displayed similar dose–response of EGF-induced receptor tyrosine phosphorylation and activation of MAPK and AKT.

binding was allowed to proceed to equilibrium at 25°C for 1 h. Cells were then washed in cold PBS and lysed in 0.5 M NaOH overnight at 25°C. A portion of each sample was then counted in a liquid scintillation counter for 10 min. Binding data were analyzed by the method of Scatchard using PRISM software (GraphPad, San Diego) (14).

Measurement of Dissociation Rates. Cells were plated for binding and washed as described above. Duplicate wells were incubated with a single concentration of ^{125}I-EGF at 4°C for 2.5 h. Cells were then washed twice in cold DMEM containing 0.1% BSA, and the final wash allowed to remain on the cells for varying times ranging from 2 min to 3 h. After the dissociation period, cells were washed in PBS and lysed as described above, and a portion of each sample was counted in the liquid scintillation counter. Binding data were analyzed by performing nonlinear regression using a one-phase exponential decay equation using PRISM software.

Results and Discussion

We have tested the mechanism proposed by the structural studies by comparing the binding characteristics and cellular signaling via EGFRs mutated in the autoinhibitory domain II/IV tether and in the dimerization arm in domain II that are expressed in 3T3-derived cells (2.2 clone) deficient in EGFR (12).

Release of the Tethered Configuration of the EGFR. To examine the role of the intramolecular domain II/IV tether in autoinhibition of the EGFR and to investigate its effects on the receptor's ligand-binding properties we generated three separate mutants in which the region of domain IV that participates in the intramolecular II/IV tether is altered. Based on the crystal structures of the unliganded EGFR and ErbB3 extracellular regions each of these mutations is predicted to disrupt intramolecular autoinhibitory contacts (6, 7). Residues in this region of domain IV were mutated to their counterparts in ErbB2, which does not form the intramolecular tether (10, 15). The G564P mutation is predicted to significantly alter the backbone configuration in the region of domain IV that interacts with the domain II dimerization arm, thus disrupting several intramolecular interactions. The H566F mutation removes at least one of just four (or five) hydrogen bonds from the domain II/IV interaction and will thus compromise the tether. The deletion mutant Δ560-590 removes the entire tethering portion of domain IV (Fig. 1 *Upper*). Each of these mutant receptors was cloned into a retroviral vector and stable cell lines were generated. Cell lines that were matched for similar levels of receptor expression (200,000–300,000 receptors per cell) were then selected for further analysis. Surface expression of each receptor version in each of the cell lines used for these experiments was confirmed by fluorescence-activated cell sorting analysis of cells fluorescently labeled with anti-EGFR antibodies (data not shown).

Effects of Disrupting the Intramolecular Tether on EGF Binding. To determine whether the intramolecular autoinhibitory tether contacts would influence the ligand binding characteristics of the receptors we performed quantitative ^{125}I-EGF bnding experiments in cells stably expressing wild-type and tether-mutated EGFR. As described above, the EGFR exists in two affinity states on the cell surface based on the concave-up plots generated by Scatchard analysis of ^{125}I-EGF binding experiments carried out on intact cells. The initial steep slope of this curve is generally interpreted to represent a small population (≈5%) of high-affinity receptors, whereas the shallow slope corresponds to a majority (≈95%) population of EGFRs that bind EGF with low-affinity (3). As shown in Fig. 1 *Middle Left*, the wild-type receptor expressed in this cellular context exhibits the classical Scatchard plot with two apparent affinity classes. Based on the hypothesis outlined above, we expected that disrupting the

autoinhibitory tether would give a receptor with higher EGF-binding affinity, or alternatively that an increased fraction of receptors would exist in the high-affinity class. In contrast to our expectations, the ligand-binding characteristics of the G564P mutant appear essentially identical to the wild-type receptor (Fig. 1 *Middle Right*). Although the two cell types express different amounts of EGFR, the ratio between the high- and low-affinity receptors between these two cell lines is similar. Approximately 4% of the receptors exhibit high-affinity and 96% exhibit low-affinity binding. Interestingly, the other two mutants, H566F and Δ560-590, gave Scatchard plots that cannot be characterized by either one-site or two-site binding (Fig. 1 *Bottom*). Scatchard plots with similar shape have also been seen for other EGFR mutants and were interpreted as having lost the high-affinity binding (9). Simple loss of high-affinity binding however, should produce a linear Scatchard plot with a slope corresponding to the low-affinity K_d. Because mutations that disrupt the intramolecular tether have been shown to increase (by ≈4-fold) rather than decrease affinity of ligand binding to the soluble forms of the EGFR extracellular region (7, 16), we are reluctant to interpret the complex curves seen in Fig. 1 for the H566F and Δ560-590 mutants as a simple loss of high-affinity binding. Rather, we believe that clear conclusions regarding binding affinity of full-length receptors in intact cells cannot be drawn from this line of experimentation. We suggest that ^{125}I-EGF binding experiments in intact cells are dependent on factors such as receptor clustering, sequestration in coated pits, and receptor internalization so that a simple molecular interpretation is not possible.

We next compared the rate of EGF dissociation for the wild-type receptor and for each of the receptor tether mutants. A fixed concentration of ^{125}I-labeled EGF was allowed to bind to cells at 4°C until equilibrium was reached, and dissociation of bound ligand was then monitored by measuring what remained at different times. The G564P, H566F, and Δ560-590 mutants all consistently displayed dissociation rates that were similar to or slower than the wild-type EGFR (Fig. 2). It is possible that the H566F mutant adopts a conformation more similar to the extended EGFR configuration, thus accounting for its significantly decreased EGF dissociation rate. This experiment suggests that EGF dissociates from receptors in the extended configuration more slowly than from the tethered configuration, implying that the extended configuration binds EGF with higher affinity. These results are consistent with the model for binding affinity and receptor activation implied by the EGFR crystal structures. Formation of the intramolecular domain II/IV tether prevents the ligand binding domains I and III from coming sufficiently close to one another for both of them to be able to contact the same bound ligand. When the autoinhibitory tether is released by mutation or deletion, the receptor is free to adopt the extended conformation in which domains I and III can assume their optimal positions for high-affinity binding to EGF and thus reduce the rate of ligand dissociation.

Effects of Disrupting the Intramolecular Tether on Signals by EGFR. We next examined the biochemical responses of the G564P, H566F, and the Δ560-590 mutants to EGF stimulation, by comparing the dose–response and kinetics of EGFR activation and signaling. Serum-starved cells were treated either with a single concentration of EGF for varying periods of time (Fig. 3*A*) or with varying concentrations of EGF for a fixed time (Fig. 3*B*). These experiments showed that mutations in the tether-forming region of domain IV exhibit kinetics of receptor activation and a dose–response relationship very similar to those obtained for wild-type EGFR for all signaling outputs tested. The Δ560-590 mutant reproducibly displayed slightly delayed kinetics of EGF-mediated stimulation of autophosphorylation and activation of AKT and MAPK. Additionally, both the Δ560-590 and H566F mutants appeared to require somewhat higher concentrations of EGF than wild-type EGFR to promote a similar AKT response.

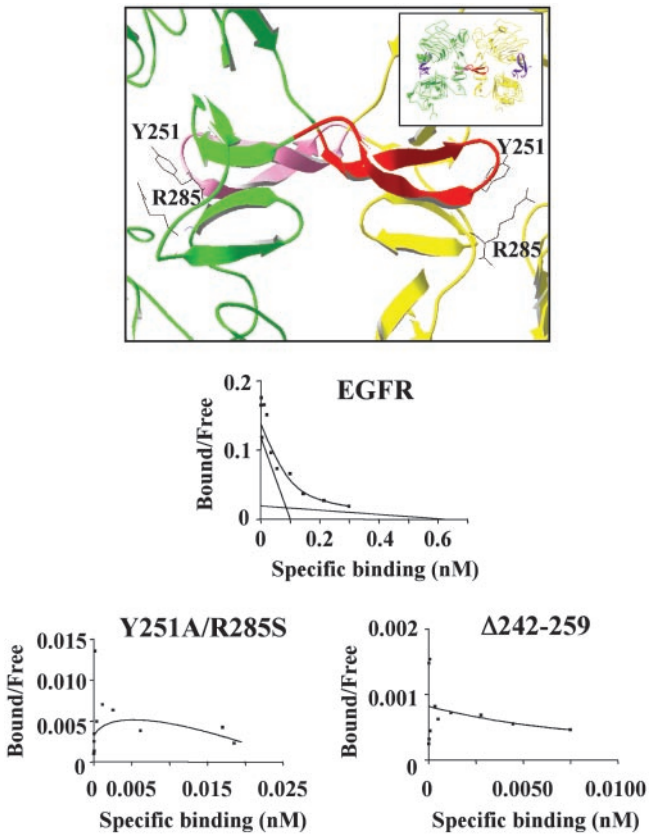

Fig. 4. EGF-binding characteristics of EGFRs mutated in the dimerization arm in domain II. Cells expressing wild-type EGFR or receptors with mutations in the dimerization arm of domain II were grown to confluence in 24-well plates and incubated with increasing concentrations of ^{125}I-EGF in triplicate for 60 min at room temperature. A 100-fold excess of unlabeled EGF was simultaneously added to the third well to determine nonspecific binding. Scatchard plots are shown for cell lines expressing wild-type EGFR, Y251A/R285S, and the Δ242-259 deletion mutant of EGFR. Mutagenic disruption of the dimerization arm of domain II led to a dramatic change in the Scatchard curves that was inconsistent with two classes of EGF-binding affinity. A ribbon diagram of the structure of the dimerization arm of domain II of the EGFR is shown (*Top*), with the complete dimeric EGFR extracellular domain structure (*Inset*). The dimerization arm (residues 242–259) of one receptor protomer is shown in red, and the dimerization arm of the other protomer is shown in pink. EGF is shown in purple (*Inset*) (PDB accession no. 1IVO; ref. 8).

The most important finding, however, is that despite having mutations that should disrupt the proposed autoinhibitory tether, none of the mutants that we analyzed displayed any significant level of receptor autophosphorylation or activation of downstream signaling proteins in the absence of EGF. We would expect to see both if release of an autoinhibitory intramolecular tether yielded a constitutively active receptor (Fig. 3). Taken together, these experiments argue that the autoinhibition conferred by the domain II/IV tether is subtle at best, and that the maintenance of EGFR in its inactive state must also involve additional mechanisms.

Effects of Disrupting the Dimerization Arm of the EGFR. To examine the role of the dimerization arm in activation of the EGFR and to investigate how dimerization affects EGF binding, we generated a pair of mutants in this region of domain II. The crystal structures of ligand-bound EGFR suggested that the Y251A/R285S double mutant should disrupt specific hydrogen bonds

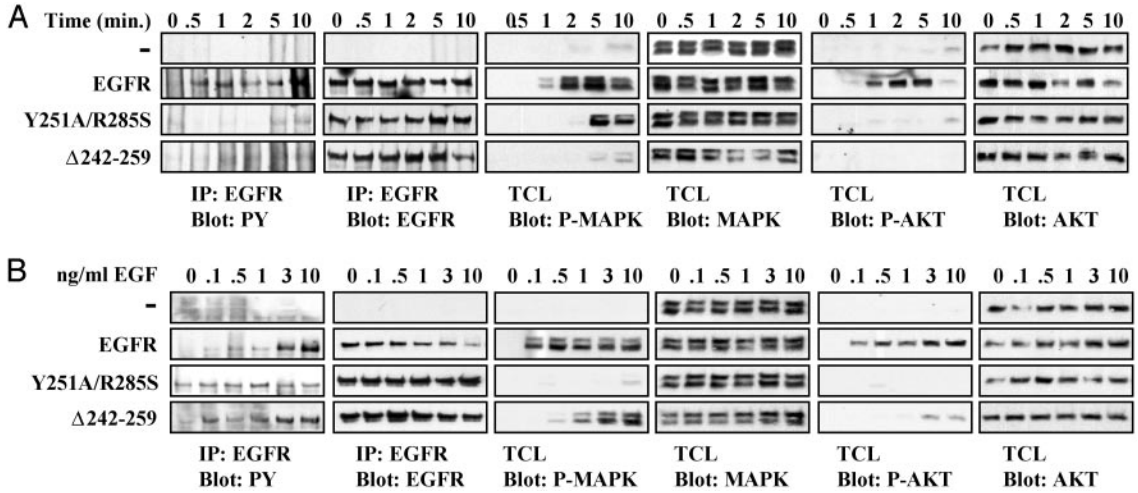

Fig. 5. Mutations in the dimerization arm of EGFR in domain II impairs signaling by means of EGFRs. (*A*) Cells expressing empty vector (−), wild-type EGFR, or the domain II mutants Y251A/R285S and the Δ242-259 deletion mutant were starved overnight and stimulated with 1 ng/ml EGF for increasing periods of time. Cell extracts were prepared and analyzed for receptor tyrosine phosphorylation and activation of MAPK and AKT by immunoblotting with antibodies that recognize specifically the activated forms of MAPK and AKT, respectively. Mutagenic disruption of the dimerization arm in domain II dramatically reduced the kinetics of tyrosine autophosphorylation of EGFR as well as activation of MAPK and AKT responses. (*B*) Cells expressing empty vector (−), wild-type EGFR, or the domain II Y251A/R285S mutants and the Δ242-259 deletion mutant were starved overnight and stimulated with increasing concentrations of EGF for 5 min at 37°C. Cell extracts were prepared and analyzed for tyrosine autophosphorylation of EGFR and activation of MAPK and AKT by immunoblotting with antibodies that recognize specifically the activated forms of MAPK and AKT, respectively. The dimerization arm mutant Y251A/R285S was essentially defective for EGF-induced receptor tyrosine phosphorylation as well as for MAPK and AKT activation at all EGF concentrations tested. The deletion mutant Δ242-259 required higher concentrations of EGF to induce activation of MAPK and AKT relative to activation of MAPK or AKT after activation of wild-type EGFR.

and hydrophobic interactions across the interface of the EGFR dimer. In addition, we generated an EGFR deletion mutant (Δ242-259) that lacks the entire dimerization arm of domain-II (Fig. 4 *Top*). Similar mutations have been described, but were not rigorously examined either for their ligand-binding characteristics or for EGF-mediated receptor activation (8, 9). We cloned these mutant receptors into a retroviral vector, and generated stable cell lines by selection for cotransduction of an antibiotic resistance gene. Cell lines screened for similar levels of receptor expression were then used in subsequent experiments. Surface expression of each mutant was confirmed by fluorescence-activated cell sorting analysis of cells labeled with anti-EGFR antibodies.

We first analyzed binding of ^{125}I-labeled EGF to cells expressing these mutants. Similar to our findings with the H566F and Δ560-590 mutants, the two dimerization arm mutants produced Scatchard plots that could not be characterized by one-site or two-site binding (Fig. 4 *Bottom*). We therefore examined the effects of dimerization site mutants on the rate of EGF dissociation, as described above, to evaluate their ligand binding. As shown in Fig. 2, interestingly, both the Y251A/R285S mutant and the Δ242-259 deletion mutant reproducibly exhibited an increased rate of EGF dissociation (i.e., reduced half-life) relative to the dissociation rate from wild-type EGFR, suggesting that dimerization stabilizes the interaction between the EGFR and EGF. The results presented here suggest that the ligand dissociation rate makes an important contribution to the overall affinity of EGF toward EGFR and that receptor conformation affects this dissociation rate.

Impaired Cell Signaling in Cells Expressing Dimerization-Arm EGFR Mutants. We next examined the biochemical response of the dimerization arm mutants to EGF stimulation by exploring the dose-response and kinetics of EGFR activation and signaling via EGFR in the context of disrupted dimerization. These experiments highlight the essential role of residues in the dimerization arm, as these receptor mutants showed significantly impaired autophosphorylation and stimulation of signaling. As shown in Fig. 5, both the Y251A/R285S and the Δ242-259 deletion mutants displayed markedly reduced EGFR autophosphorylation after EGF stimulation at all times and concentrations tested. Although we did observe basal receptor autophosphorylation, these receptors are clearly defective for cell signaling. Activation of the MAPK response is virtually absent at all EGF concentrations tested for the Y251A/R285S mutant. Additionally, this receptor requires a significantly prolonged period of stimulation to achieve a weak MAPK phosphorylation. Deletion of the key contact residues in the dimerization arm (Δ242-259) generated a receptor that required higher concentrations of EGF and longer periods of EGF stimulation to achieve significant activation of MAPK. In addition, neither of these mutants induced activation of the AKT-dependent cell survival pathway in response to EGF stimulation (Fig. 5).

Conclusions

Studies of EGF binding to intact cells that express EGFRs typically give rise to Scatchard plots with concave-up curvature. The prevailing model holds that the initial steep slope of this curve directly represents a small population of high-affinity receptors, whereas the subsequent shallow slope of the curve represents a majority of EGFRs that bind EGF with only low affinity. An attractive hypothesis based on the x-ray crystal structures of unliganded EGFR and ErbB3 extracellular domains was that the high-affinity receptors might correspond to the extended active configuration, whereas the low-affinity receptors might represent the tethered, autoinhibited configuration (4, 6–9). We have tested this hypothesis by using intact mutated receptors expressed at the cell surface, and find that disruption of the autoinhibitory tether does not give rise to a single receptor population that binds ligand with high affinity, and neither does disruption of receptor dimerization yield a receptor that binds EGF with only a single low affinity, as might be anticipated in the simplest case. Indeed efforts by a number of groups to mathematically model the consistently observed

concave-up curvature of the EGFR Scatchard plot based on a receptor with two affinity states have been unsuccessful (17–19). As described in detail in the accompanying paper (11), it is possible to model the concave-up curvature in the context of ligand-mediated receptor dimerization only if ligand-bound dimers are allowed to bind with high affinity to a saturatable "external site," possibly representing receptors sequestered in coated pits or other structures before receptor internalization. According to our current model, the initial steep slope observed in Scatchard plots represents dimerized ligand-bound EGFRs that have undergone a high-affinity association with this external site. The subsequent shallow slope of the Scatchard curve then represents a dynamically exchanging population of EGFRs on the cell surface that continuously sample the tethered, autoinhibitory conformation that binds EGF with lower affinity, and the ensemble of extended conformations (including that competent to dimerize) that bind EGF with higher affinity.

Although EGFRs with mutations in the tether region display a decreased rate of EGF-dissociation, implying that relief of the autoinhibitory tether configuration does alter ligand receptor interactions, the effects are small and cannot account for the overall inactive state of the EGFR in quiescent cells before ligand stimulation. In other words, our experiments show that the autoinhibited configuration of the extracellular ligand binding region of EGFR provides only limited control of EGFR activation. We have previously proposed that the sensitivity of the EGFR and other receptor tyrosine kinases (RTKs) as signaling systems is increased by possessing multiple mechanisms for autoinhibition that have evolved to fulfill the conflicting requirements for sensitivity versus background noise (20). It has been shown that the protein tyrosine kinase activity (PTK) of RTKs can be autoinhibited by additional constraints mediated by the transmembrane domain (21), juxtamembrane region (22), by the activation loop of the catalytic PTK core (23) as well as the C-terminal tail containing the tyrosine autophosphorylation sites (24, 25). In addition, there is good evidence that protein tyrosine phosphatases continuously monitor the activity of RTKs in unstimulated cells by dephosphorylating phosphotyrosines in the PTK domain that have become phosphorylated as a consequence of leakiness (or noise) in RTK autoinhibition (26, 27). Indeed, at high levels of RTK expression, such as in cancer cells, where cell transformation is driven by overexpression of EGFR or ErbB2, ligand-independent autophosphorylation of these receptors can lead to receptor activation and cell transformation (2). Nature has thus designed a system in which a series of independent mechanisms allow the cell to exert very precise control over the level of EGFR signaling at normal levels of receptor expression without compromising sensitivity.

This work was supported in part by a James Hudson Brown–Alexander B. Coxe Postdoctoral Fellowship (to D.M.) and by National Cancer Institute Grant R01-CA79992 (to M.A.L.).

1. Jorissen, R. N., Walker, F., Pouliot, N., Garrett, T. P., Ward, C. W. & Burgess, A. W. (2003) *Exp. Cell Res.* **284,** 31–53.
2. Blume-Jensen, P. & Hunter, T. (2001) *Nature* **411,** 355–365.
3. Lax, I., Bellot, F., Howk, R., Ullrich, A., Givol, D. & Schlessinger, J. (1989) *EMBO J.* **8,** 421–427.
4. Schlessinger, J. (2002) *Cell* **110,** 669–672.
5. Schlessinger, J. (2000) *Cell* **103,** 211–225.
6. Cho, H. S. & Leahy, D. J. (2002) *Science* **297,** 1330–1333.
7. Ferguson, K. M., Berger, M. B., Mendrola, J. M., Cho, H. S., Leahy, D. J. & Lemmon, M. A. (2003) *Mol. Cell* **11,** 507–517.
8. Ogiso, H., Ishitani, R., Nureki, O., Fukai, S., Yamanaka, M., Kim, J. H., Saito, K., Sakamoto, A., Inoue, M., Shirouzu, M. & Yokoyama, S. (2002) *Cell* **110,** 775–787.
9. Garrett, T. P., McKern, N. M., Lou, M., Elleman, T. C., Adams, T. E., Lovrecz, G. O., Zhu, H. J., Walker, F., Frenkel, M. J., Hoyne, P. A., *et al.* (2002) *Cell* **110,** 763–773.
10. Burgess, A. W., Cho, H. S., Eigenbrot, C., Ferguson, K. M., Garrett, T. P., Leahy, D. J., Lemmon, M. A., Sliwkowski, M. X., Ward, C. W. & Yokoyama, S. (2003) *Mol. Cell* **12,** 541–552.
11. Klein, P., Mattoon, D., Lemmon, M. A. & Schlessinger, J. (2003) *Proc. Natl. Acad. Sci. USA* **101,** 929–934.
12. Honegger, A. M., Szapary, D., Schmidt, A., Lyall, R., Van Obberghen, E., Dull, T. J., Ullrich, A. & Schlessinger, J. (1987) *Mol. Cell. Biol.* **7,** 4568–4571.
13. Batzer, A. G., Rotin, D., Urena, J. M., Skolnik, E. Y. & Schlessinger, J. (1994) *Mol. Cell. Biol.* **14,** 5192–5201.
14. Scatchard, G. (1949) *Ann. N.Y. Acad. Sci.* **51,** 660–672.
15. Cho, H. S., Mason, K., Ramyar, K. X., Stanley, A. M., Gabelli, S. B., Denney, D. W., Jr., & Leahy, D. J. (2003) *Nature* **421,** 756–760.
16. Elleman, T. C., Domagala, T., McKern, N. M., Nerrie, M., Lonnqvist, B., Adams, T. E., Lewis, J., Lovrecz, G. O., Hoyne, P. A., Richards, K. M., *et al.* (2001) *Biochemistry* **40,** 8930–8939.
17. Wofsy, C. & Goldstein, B. (1992) *Math. Biosci.* **112,** 115–154.
18. Holbrook, M. R., Slakey, L. L. & Gross, D. J. (2000) *Biochem. J.* **352,** 99–108.
19. Lemmon, M. A., Bu, Z., Ladbury, J. E., Zhou, M., Pinchasi, D., Lax, I., Engelman, D. M. & Schlessinger, J. (1997) *EMBO J.* **16,** 281–294.
20. Schlessinger, J. (2003) *Science* **300,** 750–752.
21. Fleishman, S. J., Schlessinger, J. & Ben-Tal, N. (2002) *Proc. Natl. Acad. Sci. USA* **99,** 15937–15940.
22. Wybenga-Groot, L. E., Baskin, B., Ong, S. H., Tong, J., Pawson, T. & Sicheri, F. (2001) *Cell* **106,** 745–757.
23. Hubbard, S. R., Wei, L., Ellis, L. & Hendrickson, W. A. (1994) *Nature* **372,** 746–754.
24. Honegger, A., Dull, T. J., Bellot, F., Van Obberghen, E., Szapary, D., Schmidt, A., Ullrich, A. & Schlessinger, J. (1988) *EMBO J.* **7,** 3045–3052.
25. Honegger, A., Dull, T. J., Szapary, D., Komoriya, A., Kris, R., Ullrich, A. & Schlessinger, J. (1988) *EMBO J.* **7,** 3053–3060.
26. Tonks, N. K. & Neel, B. G. (2001) *Curr. Opin. Cell Biol.* **13,** 182–195.
27. Elchebly, M., Payette, P., Michaliszyn, E., Cromlish, W., Collins, S., Loy, A. L., Normandin, D., Cheng, A., Himms-Hagen, J., Chan, C. C., *et al.* (1999) *Science* **283,** 1544–1548.